American Mineralogist, Volume 97, pages 197–202, 2012

Markascherite, $Cu_3(MoO_4)(OH)_4$, a new mineral species polymorphic with szenicsite, from Copper Creek, Pinal County, Arizona, U.S.A.

H. YANG,* R.A. JENKINS, R.M. THOMPSON, R.T. DOWNS, S.H. EVANS, AND E.M. BLOCH

Department of Geosciences, University of Arizona, 1040 East 4th Street, Tucson, Arizona 85721, U.S.A.

ABSTRACT

A new mineral species, markascherite (IMA2010-051), ideally $Cu_3(MoO_4)(OH)_4$, has been found at Copper Creek, Pinal County, Arizona, U.S.A. The mineral is of secondary origin and is associated with brochantite, antlerite, lindgrenite, wulfenite, natrojarosite, and chalcanthite. Markascherite crystals are bladed (elongated along the **b** axis), up to 0.50 × 0.10 × 0.05 mm. The dominant forms are {001}, {100}, and {010}. Twinning is found with the twofold twin axis along $[10\bar{1}]$. The mineral is green, transparent with green streak and vitreous luster. It is brittle and has a Mohs hardness of 3.5~4; cleavage is perfect on {100} and no parting was observed. The calculated density is 4.216 g/cm^3. Optically, markascherite is biaxial (–), with n_α >1.8, n_β > 1.8, and n_γ >1.8. The dispersion is strong ($r > v$). It is insoluble in water, acetone, or hydrochloric acid. An electron microprobe analysis yielded an empirical formula $Cu_{2.89}(Mo_{1.04}O_4)(OH)_4$.

Markascherite, polymorphic with szenicsite, is monoclinic, with space group $P2_1/m$ and unit-cell parameters a = 9.9904(6), b = 5.9934(4), c = 5.5255(4) Å, β = 97.428(4)°, and V = 328.04(4) Å^3. Its structure is composed of three nonequivalent, markedly distorted $Cu^{2+}(O,OH)_6$ octahedra and one MoO_4 tetrahedron. The Cu1 and Cu2 octahedra share edges to form brucite-type layers parallel to (100), whereas the Cu3 octahedra share edges with one another to form rutile-type chains parallel to the b axis. These layers and chains alternate along [100] and are interlinked together by both MoO_4 tetrahedra and hydrogen bonds. Topologically, the structure of markascherite exhibits a remarkable resemblance to that of deloryite, $Cu_4(UO_2)(MoO_4)_2(OH)_6$, given the coupled substitution of $[2Cu^{2+} + 2(OH^-)]^{2+}$ for $[(U^{6+} + \square) + 2O^{2-}]^{2+}$. The Raman spectra of markascherite are compared with those of two other copper molybdate minerals szenicsite and lindgrenite.

Keywords: Markascherite, szenicsite, molybdate, copper oxysalt, crystal structure, X-ray diffraction, Raman spectra

INTRODUCTION

A new mineral species, markascherite, ideally $Cu_3(MoO_4)(OH)_4$, has been found at Copper Creek, Pinal County, Arizona, U.S.A. It is dimorphic with szenicsite (Francis et al. 1997) and is named after its finder, Mark Goldberg Ascher, a mineral collector and engineer in Tucson, Arizona. The new mineral and its name have been approved by the Commission on New Minerals, Nomenclature and Classification (CNMNC) of the International Mineralogical Association (IMA2010-051). A part of the cotype sample has been deposited at the University of Arizona Mineral Museum (catalog 19291) and a part is in the RRUFF Project (deposition R100030).

Hydroxyl copper molybdates are not common in nature. In addition to szenicsite and markascherite, four other minerals may be classified into this category, including lindgrenite $Cu_3(MoO_4)_2(OH)_2$, deloryite $Cu_4(UO_2)Mo_2O_8(OH)_6$, molybdofornacite $CuPb_2MoO_4AsO_4(OH)$, and obradovicite $H_4KCuFe^{3+}_2(AsO_4)(MoO_4)_5 \cdot 12H_2O$. Despite their relative rarity in nature, hydroxyl copper molybdates have attracted considerable attention recently owing to their promising applications in various fields, such as organic-inorganic hybrid materials, catalysts, adsorption, electrical conductivity, magnetism, photochemistry, sensors, solid-state electrolytes, and energy storage (e.g., Xu et al. 1999; Tian et al. 2004; Pavani and Ramanan 2005; Pavani et al. 2006, 2009, 2011; Vilminot et al. 2006; Xu and Xue 2007; Montney et al. 2009; Alam and Feldmann 2010; Mitchell et al. 2010). In particular, lindgrenite has been synthesized under hydrothermal conditions for studies on its morphological architecture, structural, and magnetic properties, thermal behaviors, and catalytic effects (Pavani and Ramanan 2005; Bao et al. 2006; Vilminot et al. 2006; Xu and Xue 2007). Furthermore, a triclinic $Cu_3(MoO_4)_2(OH)_2$ phase, dimorphic with lindgrenite, has also been synthesized hydrothermally (Xu et al. 1999). In this paper, we describe the physical and chemical properties of markascherite and its structural relationships with other hydroxyl copper molybdates based on single-crystal X-ray diffraction and Raman spectroscopic data.

SAMPLE DESCRIPTION AND EXPERIMENTAL METHODS

Occurrence, physical, and chemical properties, and Raman spectra

Markascherite was found in material collected from the surface of the south glory hole of the Childs Aldwinkle mine in the Galiuro Mountains, Bunker Hill District, Copper Creek, Pinal County, Arizona, U.S.A. (lat. 32°45′07″ N and long. 110°28′55″). The south glory hole is the top of a breccia pipe. Associated minerals include brochantite, $Cu_4SO_4(OH)_6$, on a brecciated quartz matrix. The mineral is of secondary origin from the breakdown of primary molybdenite

* E-mail: hyang@u.arizona.edu

MoS_2, bornite Cu_5FeS_4, chalcocite Cu_2S, and chalcopyrite $CuFeS_2$, all of which are present in the south glory hole. Other minerals found in the south glory hole include antlerite $Cu_3(SO_4)(OH)_4$, lindgrenite $Cu_3(MoO_4)_2(OH)_2$, wulfenite $PbMoO_4$, natrojarosite $NaFe_3^{3+}(SO_4)_2(OH)_6$, and chalcanthite $CuSO_4{\cdot}5H_2O$. Markascherite crystals are bladed (elongated along the **b** axis), up to 0.50 × 0.10 × 0.05 mm (Fig. 1). The dominant forms are {001}, {100}, and {010}. Twinning is found with the twofold twin axis along [10$\bar{1}$]. The mineral is green, transparent with green streak and subadamantine luster. It is brittle and has a Mohs hardness of 3.5~4; cleavage is perfect on {100} and no parting was observed. The calculated density is 4.216 g/cm^3 using the empirical formula, which is less than that calculated for szenicsite (~4.280 cm^3) using data from Burns (1998) and Stolz and Armbruster (1998). Optically, markascherite is biaxial (–), with n_α >1.8, n_β > 1.8, and n_γ >1.8. The dispersion is strong (r > v). It is insoluble in water, acetone, or hydrochloric acid.

The chemical composition was determined with a CAMECA SX50 electron microprobe at 15 kV and 20 nA. The standards used include chalcopyrite for Cu and $CaMoO_4$ for Mo, yielding an average composition (wt%) (13 points) of CuO 54.99(47), MoO_3 35.17(43), and total = 90.16(64). The theoretical content of H_2O is 8.61% from the ideal formula (see below). The resultant chemical formula, calculated on the basis of 8 O atoms (from the structure determination), is $Cu_{2.89}(Mo_{1.04}O_4)(OH)_4$, which can be simplified as $Cu_3(MoO_4)(OH)_4$.

The Raman spectra of markascherite, along with those of szenicsite and lindgrenite (RRUFF deposition R050146 and R060241, respectively) for comparison, were collected on a randomly oriented crystal from 9 scans at 30 s and 200 mW power per scan on a Thermo Almega microRaman system, using a solid-state laser with a frequency of 532 nm and a thermoelectrically cooled CCD detector. The laser is partially polarized with 4 cm^{-1} resolution and a spot size of 1 μm.

X-ray crystallography

Because of the limited amount of available material, no powder X-ray diffraction data were measured for markascherite. Listed in Table 1 are the powder X-ray diffraction data calculated from the determined structure using the program XPOW (Downs et al. 1993). Single-crystal X-ray diffraction data of markascherite were collected from a nearly equi-dimensional, untwinned crystal (0.04 × 0.05 × 0.05 mm) on a Bruker X8 APEX2 CCD X-ray diffractometer equipped with graphite-monochromatized Mo$K\alpha$ radiation with frame widths of 0.5° in ω and 30 s counting time per frame. All reflections were indexed on the basis of a monoclinic unit cell (Table 2). The intensity data were corrected for X-ray absorption using the Bruker program SADABS. The systematic absences of reflections suggest possible space group $P2_1$ (no. 4) or $P2_1/m$ (no. 11). The crystal structure was solved from the direct method and refined using SHELX97 (Sheldrick 2008) based on the space group $P2_1/m$, because it yielded the better refinement statistics in terms of bond lengths and angles, atomic displacement parameters, and R factors. The detailed structure refinement procedures were similar to those described by Yang et al. (2011). The positions of all atoms were refined with anisotropic displacement parameters, except for H atoms, which were refined with a fixed isotropic displacement parameter (U_{eq} = 0.03). The ideal chemistry, $Cu_3(MoO_4)(OH)_4$, was assumed during the structure refinements, because an exploratory refinement showed that all Cu sites were nearly fully occupied, contrasting the slightly low Cu total from the electron microprobe analysis. Final coordinates and displacement parameters of atoms in markascherite are listed in Table 3, and selected bond distances in Table 4.

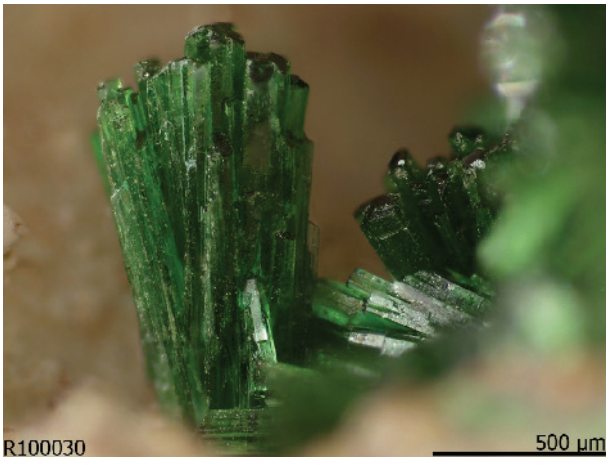

FIGURE 1. Photograph of markascherite crystals. (Color online.)

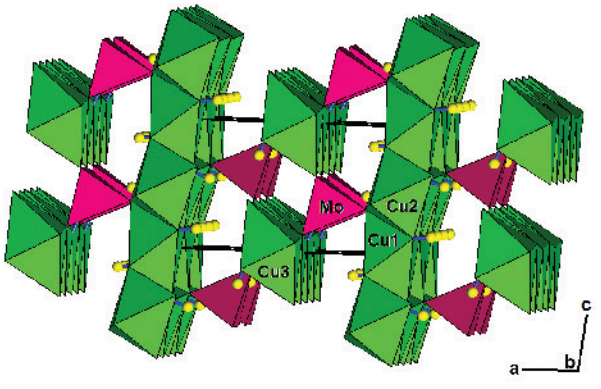

FIGURE 2. Crystal structure of markascherite. Tetrahedra = MoO_4 groups and octahedra = $Cu(O,OH)_6$. Small spheres represent H atoms. (Color online.)

TABLE 1. Calculated powder X-ray diffraction data for markascherite

Intensity	d_{calc}	h k l	Intensity	d_{calc}	h k l
22	9.896	0 0 1	2	1.876	$\bar{1}$ 3 0
5	5.472	1 0 0	1	1.870	$\bar{2}$ 1 4
65	**5.124**	**0 1 1**	11	1.861	$\bar{1}$ 2 4
100	**4.948**	**0 0 2**	2	1.852	0 3 2
10	4.040	$\bar{1}$ 1 0	4	1.850	$\bar{1}$ 1 5
21	3.938	$\bar{1}$ 0 2	5	1.828	1 3 1
15	3.875	$\bar{1}$ 1 1	18	1.810	$\bar{2}$ 2 2
24	3.815	0 1 2	10	1.803	$\bar{2}$ 2 3
34	3.619	1 1 1	4	1.781	$\bar{1}$ 3 2
54	**3.450**	**1 0 2**	5	1.753	3 0 1
51	**3.299**	**0 0 3**	2	1.745	3 1 0
31	3.290	$\bar{1}$ 1 2	17	1.725	$\bar{2}$ 0 4
53	**3.006**	**$\bar{1}$ 0 3**	4	1.715	$\bar{3}$ 1 2
2	2.995	0 2 0	2	1.694	$\bar{3}$ 0 3
4	2.990	1 1 2	1	1.682	3 1 1
2	2.890	0 1 3	1	1.658	2 1 4
55	**2.736**	**2 0 0**	9	1.649	0 0 6
2	2.731	$\bar{2}$ 0 1	2	1.649	$\bar{2}$ 1 5
11	2.673	1 0 3	6	1.645	$\bar{2}$ 2 4
88	**2.580**	**$\bar{1}$ 2 1**	1	1.643	$\bar{3}$ 0 2
24	2.562	0 2 2	2	1.640	$\bar{1}$ 0 6
4	2.552	2 0 1	27	1.631	$\bar{1}$ 2 5
6	2.489	2 1 0	2	1.630	$\bar{3}$ 1 3
3	2.441	$\bar{1}$ 1 3	3	1.613	2 3 0
8	2.384	$\bar{1}$ 2 2	2	1.600	1 3 3
4	2.375	$\bar{1}$ 0 4	1	1.573	$\bar{2}$ 3 1
4	2.348	$\bar{2}$ 1 1	3	1.571	$\bar{3}$ 0 4
10	2.339	$\bar{2}$ 1 2	2	1.570	$\bar{2}$ 3 2
5	2.287	0 1 4	**51**	**1.566**	**$\bar{3}$ 2 1**
35	2.271	2 0 2	3	1.558	3 2 0
14	2.262	$\bar{1}$ 2 2	2	1.554	0 3 4
9	2.257	$\bar{2}$ 0 3	42	1.535	1 2 5
11	2.217	0 2 3	3	1.513	$\bar{3}$ 2 1
3	2.208	$\bar{1}$ 1 4	18	1.503	$\bar{2}$ 0 6
5	2.150	$\bar{1}$ 0 4	23	1.498	0 4 0
60	**2.122**	**$\bar{1}$ 2 3**	3	1.488	$\bar{2}$ 2 5
1	2.112	$\bar{2}$ 1 3	1	1.477	$\bar{1}$ 1 6
5	2.024	1 1 4	9	1.474	$\bar{3}$ 2 3
6	1.994	1 2 3	1	1.468	3 1 3
7	1.981	2 0 3	2	1.463	1 3 4
4	1.957	0 3 1	8	1.440	3 2 2
12	1.942	2 2 1	5	1.433	0 4 2
5	1.881	2 1 3	2	1.406	$\bar{2}$ 3 3
3	1.879	0 1 5	1	1.400	$\bar{1}$ 4 2

TABLE 2. Summary of crystal data and refinement results for markascherite and szenicsite

	Markascherite	Szenicsite
Ideal chemical formula	$Cu_3MoO_4(OH)_4$	$Cu_3MoO_4(OH)_4$
Crystal symmetry	Monoclinic	Orthorhombic
Space group	$P2_1/m$ (no. 11)	*Pnnm* (no. 58)
a (Å)	9.9904(6)	12.559(2)
b (Å)	5.9934(4)	8.518(3)
c (Å)	5.5255(4)	6.072(1)
α (°)	90	90
β (°)	97.428(4)	90
γ (°)	90	90
V (Å^3)	328.04(4)	649.5(3)
Z	2	4
ρ_{cal} (g/cm^3)	4.216	4.279
λ (Å, Mo*K*α)	0.71073	0.71073
μ (mm^{-1})	11.46	11.57
2θ range for data collection	≤67.48	≤54.8
No. of reflections collected	4919	4834
No. of independent reflections	1376	772
No. of reflections with $I > 2\sigma(I)$	1167	712
No. of parameters refined	75	78
R_{int}	0.029	0.062
Final R_1, wR_2 factors [$I > 2\sigma(I)$]	0.026, 0.049	0.026, 0.062
Final R_1, wR_2 factors (all data)	0.036, 0.051	0.031
Goodness-of-fit	1.013	1.261
Strong powder lines	4.948(100)	2.603(100)
	2.580(88)	3.757(70)
	5.124(65)	1.524(55)
	2.122(60)	2.587(46)
	2.736(55)	5.466(41)
	3.450(54)	5.055(41)
	3.006(53)	2.770(41)
	3.299(51)	3.049(38)
Reference	This work	Stolz and Armbruster (1998)

DISCUSSION

Crystal structure

Markascherite is dimorphic with szenicsite (Burns 1998; Stolz and Armbruster 1998) (see Table 2 for the comparison of crystallographic data for the two minerals). Its structure is composed of three symmetrically nonequivalent $Cu^{2+}(O,OH)_6$ octahedra [$Cu1O(OH)_5$, $Cu2O_2(OH)_4$, and $Cu3O_4(OH)_2$] and one MoO_4 tetrahedron. The $Cu1O(OH)_5$ and $Cu2O_2(OH)_4$ octahedra share edges with each other to form brucite-type layers parallel to (100) (the cleavage plane), whereas the $Cu3O_4(OH)_2$ octahedra shares edges with one another to form rutile-type chains extending along the *b* axis (the crystal elongation direction). The rutile-type chains made of $Cu(O,OH)_6$ octahedra have also been found in many other Cu-bearing minerals, such as mixite, conichalcite, euchroite, and olivenite (see the review by Eby and Hawthorne 1993). The Cu octahedral layers and chains in markascherite are interlinked by the MoO_4 tetrahedra through shared corners, as well as by hydrogen bonds, along [100] (Fig. 2). Due to the strong Jahn-Teller effect, all three Cu-octahedra are noticeably distorted (Table 4), with four relatively short Cu-O bond distances and two long ones, giving rise to (4+2) elongated octahedral coordinations that are commonly observed in copper oxysalts (Eby and Hawthorne 1993; Burns and Hawthorne 1996). Measured in terms of the octahedral quadratic elongation (OQE) and octahedral angle variance (OAV) (Robinson et al. 1971), the Cu1 octahedron is the most distorted of the three Cu-octahedra

TABLE 3. Coordinates and displacement parameters of atoms in markascherite

Atom	*x*	*y*	*z*	U_{iso}	U_{11}	U_{22}	U_{33}	U_{23}	U_{13}	U_{12}
Cu1	–0.00037(4)	1/4	–0.00385(8)	0.0103(1)	0.0161(2)	0.0065(2)	0.0090(2)	0	0.0040(2)	0
Cu2	0	1/2	1/2	0.0098(1)	0.0139(2)	0.0074(2)	0.0086(2)	0.0009(2)	0.0039(2)	–0.0001(1)
Cu3	1/2	1/2	0	0.0130(1)	0.0125(2)	0.0114(2)	0.0163(2)	0.0002(2)	0.0071(2)	–0.0004(1)
Mo	0.32101(3)	1/4	0.42366(6)	0.0098(1)	0.0092(1)	0.0107(1)	0.0099(1)	0	0.0022(1)	0
O1	0.1432(3)	1/4	0.3533(6)	0.0138(5)	0.011(1)	0.015(1)	0.015(1)	0	0.001(1)	0
O2	0.3940(3)	1/4	0.1365(5)	0.0153(5)	0.014(1)	0.016(1)	0.017(1)	0	0.008(1)	0
O3	0.3636(2)	0.0137(3)	0.5975(4)	0.0210(4)	0.021(1)	0.020(1)	0.022(1)	0.0073(8)	0.000(1)	0.0040(7)
OH4	0.1016(3)	3/4	0.4040(5)	0.0126(5)	0.014(1)	0.009(1)	0.015(1)	0	0.001(1)	0
OH5	0.3922(3)	3/4	0.0855(6)	0.0159(5)	0.014(1)	0.018(1)	0.017(1)	0	0.007(1)	0
OH6	0.0913(2)	0.5029(3)	0.8514(4)	0.0115(4)	0.011(1)	0.011(1)	0.013(1)	0.0011(7)	0.003(1)	–0.0002(6)
H1	0.173(5)	3/4	0.44(1)	0.03						
H2	0.367(5)	3/4	0.25(1)	0.03						
H3	0.165(4)	0.516(6)	0.837(9)	0.03						

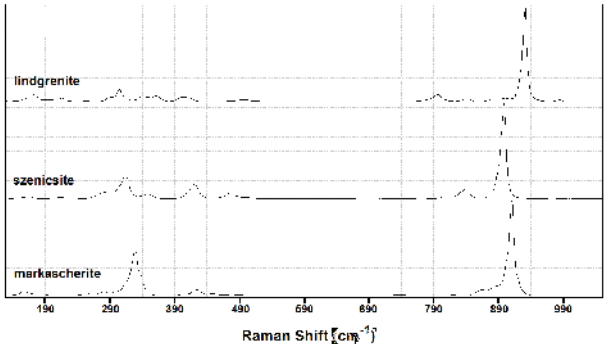

FIGURE 3. Raman spectra of markascherite, szenicsite, and lindgrenite, between 130 and 1050 cm^{-1}. The spectra are shown with vertical offset for more clarity.

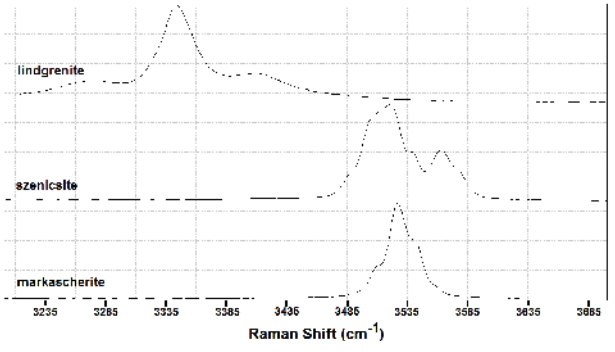

FIGURE 4. Raman spectra of markascherite, szenicsite, and lindgrenite, between 3200 and 3700 cm^{-1}. The spectra are shown with vertical offset for more clarity.

and Cu2 the least (Table 4). The average Cu-O and Mo-O distances in markascherite all fall in the ranges observed in other Cu-bearing molybdates (e.g., Hawthorne and Eby 1985; Burns 1998; Stolz and Armbruster 1998; Xu et al. 1999; Tian et al. 2004; Vilminot et al. 2006; Bao et al. 2006).

A calculation of bond-valence sums for markascherite (Table 5) using the parameters given by Brese and O'Keeffe (1991) shows that OH4 and OH6 are slightly overbonded, whereas O3 is apparently underbonded, suggesting the presence of significant hydrogen bonds between OH groups and the O3 atom. In fact, the O3 atom appears to be engaged in all possible hydrogen bonds in markascherite (Table 6), accounting for the obvious deficiency in its bond-valence sum.

Raman spectra

Numerous Raman spectroscopic studies have been conducted on various copper molybdate compounds (e.g., Maczka et al. 1999; Crane et al. 2002; Hermanowicza et al. 2006; Luz-Lima et al. 2010; Lucazeau and Machon 2006; Lucazeau et al. 2011), including hydroxyl copper molybdate minerals szenicsite and lindgrenite (Frost et al. 2004, 2007). Here, we present our Raman spectroscopic measurements on markascherite in Figures 3 and 4, along with those of szenicsite and lindgrenite. Based on previous studies on various copper molybdate minerals (Crane et al. 2002; Frost et al. 2004, 2007), we made a tentative assignment of major Raman bands for markascherite (Table 7). Evidently, the Raman spectra of markascherite, szenicsite, and lindgrenite are quite similar. In general, they can be divided into four distinct regions. Region 1, between 3230 and 3600 cm^{-1}, includes bands resulting from the O-H stretching vibrations. Region 2, between 750 and 1000 cm^{-1}, contains bands attributable to the Mo-O symmetric and anti-symmetric stretching vibrations (ν_1 and ν_3 modes) within the MoO_4 tetrahedra. Major bands in region 3, ranging from 300 to 500 cm^{-1}, are ascribed to the O-Mo-O symmetric and anti-symmetric bending vibrations (ν_2 and ν_4 modes) within the MoO_4 tetrahedra. The bands in Region 4, spanning from 130 to 310 cm^{-1}, are mainly associated with the rotational or translational modes of MoO_4 tetrahedra, as well as the lattice vibrational modes and Cu-O interactions. However, Cu2 and Cu3 do not have associated Cu-O stretching modes because they are located on inversion centers. Nonetheless, Figures 3 and 4 also reveals some spectral differences among the three minerals. For example, the wavenumber of the ν_1 mode of the MoO_4 group increases significantly from 898 cm^{-1} for szenicsite to 911 cm^{-1} for markascherite, and to 933 cm^{-1} for lindgrenite. In addition, the O-H stretching bands for lindgrenite are between 3230 and 3450 cm^{-1}, whereas those for szenicsite and markascherite range from 3460 to 3600 cm^{-1}, indicating that the O-H···O hydrogen bond lengths in lindgrenite are markedly shorter than those in szenicsite and markascherite. According to Libowitzky (1999), the O-H···O hydrogen bond lengths estimated for lindgrenite are between 2.75 and 2.90 Å and those for szenicsite and markascherite between 2.90 and 3.25 Å, in accordance with the structure determinations for these minerals (Hawthorne and Eby 1985; Burns 1998; Stolz and Armbruster 1998; Bao et al. 2006). Compared to markascherite, the O-H stretching bands for szenicsite span in a broader range, reflecting a greater variation of O-H···O hydrogen bond lengths in this mineral, which is indeed the case. The possible hydrogen bond lengths in szenicsite vary between 2.92 and 3.33 Å (Burns 1998; Stolz and Armbruster 1998), whereas those in markascherite are confined between 3.12 and 3.29 Å (Table 6).

TABLE 4. Selected bond distances in markascherite

	Distance (Å)		Distance (Å)
Cu1-OH6	1.982(2) ×2	Cu2-OH4	1.923(2) ×2
Cu1-OH6	1.991(2) ×2	Cu2-OH6	2.036(2) ×2
Cu1-O1	2.284(3)	Cu2-O1	2.291(2) ×2
Cu1-OH4	2.309(3)		
Avg.	2.090		2.083
OQE	1.041		1.018
OAV	95.5		24.4
Cu3-OH5	1.939(2) ×2	Mo-O3	1.733(2) ×2
Cu3-O2	2.036(2) ×2	Mo-O1	1.769(3)
Cu3-O3	2.455 (2) ×2	Mo-O2	1.830(3)
Avg.	2.143		1.766
OQE	1.030	TQE	1.003
OAV	29.8	TAV	7.1

TABLE 5. Calculated bond-valence sums for markascherite

	O1	O2	O3	OH4	OH5	OH6	Sum
Cu1	0.195			0.182		0.441 ×2	2.119
						0.430 ×2	
Cu2	0.191 ×2			0.517 ×2		0.381 ×2	2.178
Cu3		0.381 ×2	0.123 ×2		0.495 ×2		1.998
Mo	1.425	1.231	1.600 ×2				5.883
Sum	2.029	1.993	1.723	1.216	0.990	1.252	

TABLE 6. Possible hydrogen bonds in markascherite

D-H···A	D-H (Å)	H···A (Å)	D···A (Å)	<(DHA) (°)
O4-H1···O3	0.72(5)	2.53(4)	3.125(3)	141(1)
O5-H2···O3	1.00(6)	2.47(4)	3.285(4)	138(1)
O6-H3···O3	0.75(4)	2.53(5)	3.219(3)	153(5)

Note: D = H-donor; A = H-acceptor.

Structural relationships with other minerals and synthetic compounds

At first glance, the structure of markascherite appears to be quite different from that of its dimorph szenicsite (Burns 1998; Stolz and Armbruster 1998). In szenicsite, three distinct Cu-octahedra share edges to form triple chains (i.e., strips of three-octahedral width) running along [001], which are cross-linked by MoO_4 tetrahedra through vertex sharing. Moreover, one of the three nonequivalent Cu^{2+} cations in szenicsite (labeled as Cu2 by Stolz and Armbruster 1998 or Cu3 by Burns 1998) is solely bonded by six OH^- ions. Lindgrenite is chemically similar to markascherite and szenicsite. The $Cu(O,OH)_6$ octahedra in this mineral, however, share edges to form double chains (i.e., strips of two-octahedral width), which are cross-linked by sharing corners with MoO_4 tetrahedra (Hawthorne and Eby 1985; Bao et al. 2006; Vilminot et al. 2006).

TABLE 7. Tentative assignment of major Raman bands for markascherite

Wavenumber (cm^{-1})	Intensity	Assignment
3510, 3527, 3541, 3560	strong, sharp	O-H stretching
911	very strong, sharp	ν_1 (MoO_4) symmetric stretching
886, 864	weak, shoulder	ν_3(MoO_4)anti-symmetricstretching
402, 425, 449, 489	weak, broad	ν_4(MoO_4) anti-symmetric bending
329	strong, sharp	ν_2 (MoO_4) symmetric bending
130–310	relatively strong, sharp	Lattice vibrational modes and Cu-O interactions

However, it appears that the structure of markascherite can be transformed into that of szenicsite largely through a linear transformation, because both structures are based on the cubic close packing of O atoms. The close packed monolayers are stacked along [100] in markascherite and along [1$\bar{2}$0] in szenicsite. The major differences between two structures lie in the distributions of metal atoms (Cu and Mo). Specifically, the transformation of atomic coordinates from markascherite to szenicsite can be given as $T[v]_m + [at]_s = [v]_s$, where $[v]_m$ and $[v]_s$ represent the triple representation of a vector with respect to the markascherite and szenicsite basis vectors, respectively. T is a transformation matrix = ($\bar{1}$0½, ½0¼, 010) and t is a translation vector, where its triple with respect to the szenicsite basis is $[at]_s = [¼\ ^1/_8 0]$. Note that not all of the atoms in markascherite can be transformed in this way to the szenicsite structure, because, if they could, then the two structures would be the same. Some of the atoms also need to translate or displace to new positions. Most of the diffusion represents a shift of 0.25 along c, or a movement of ~1.5 Å.

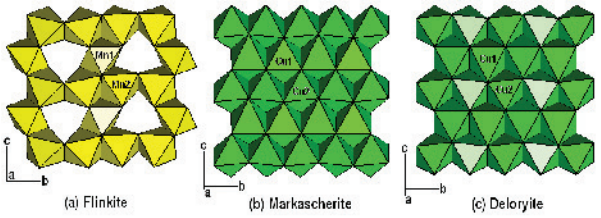

FIGURE 5. Comparison of octahedral layers in markascherite, flinkite, and deloryite. (Color online.)

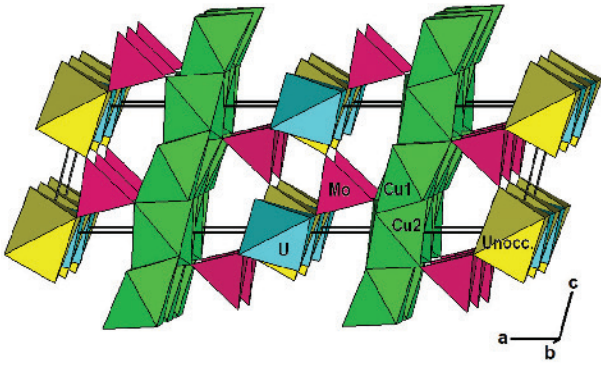

FIGURE 6. Structure of deloryite. The structure data were taken from Pushcharovsky et al. (1996). The unoccupied octahedra were indicated with the label "Unocc". (Color online.)

Listed in Table 8 are some compounds with the identical stoichiometry as markascherite, or with a general chemical formula $M_3(XO_4)(OH)_4$, where M = divalent or trivalent cations and X = tetrahedrally coordinated Mo^{6+}, S^{6+}, Se^{6+}, As^{5+}, or Si^{4+}. Yet, none of these compounds is isostructural with markascherite. The only material that contains the edge-shared octahedral layers and has the general chemical formula $M_3(XO_4)(OH)_4$ is flinkite, $Mn_2^{2+}Mn^{3+}(AsO_4)(OH)_4$ (Moore 1967; Kolitsch 2001). However, some octahedral sites within the octahedral layers are unoccupied in flinkite (Fig. 5). In other words, the octahedral layers in flinkite are not exactly the brucite-type, as those in markascherite.

Very intriguingly, the structure of markascherite exhibits a remarkable topological resemblance to that of deloryite, $Cu_4(UO_2)(MoO_4)_2(OH)_6$ (Tali et al. 1993; Pushcharovsky et al. 1996). Just like Cu1 and Cu2 in markascherite, the two distinct $Cu1O(OH)_5$ and $Cu2O_2(OH)_4$ octahedra in deloryite also share edges with each other to form the brucite-type octahedral layers parallel to (100) (Fig. 5). These octahedral layers are linked together through corner-sharing by the MoO_4 tetrahedra and distorted UO_6 octahedra. In fact, the structure of markascherite can be readily derived from that of deloryite if we double the a dimension of markascherite ($a' = 2 \times 9.99$, $b = 5.99$, $c = 5.53$ Å, and $\beta = 97.43°$ for markascherite vs. $a = 19.94$, $b = 6.12$, $c = 5.52$ Å, and $\beta = 104.18°$ for deloryite) and assume the following coupled substitution:

$$[2Cu^{2+} + 2(OH^-)]^{2+} \rightarrow [(U^{6+} + \square) + 2O^{2-}]^{2+}$$

where $\square$ stands for the vacant octahedral site (at $x = 0$, $y = ½$, $z = 0$) between two UO_6 octahedra in the deloryite, as illustrated in Figure 6. Another mineral that contains the brucite-type layers of CuO_6 octahedra is derriksite, $Cu_4(UO_2)(SeO_3)_2(OH)_6$ (Ginderow and Cesbron 1983). According to Tali et al. (1993) and Pushcharovsky et al. (1996), derriksite is structurally related to deloryite and the difference in space group between the two minerals (Table 8) is the direct consequence of the replacement of the SeO_3 trigonal pyramids in derriksite by the MoO_4 tetrahedra in deloryite.

Layered transition-metal molybdates have been a subject of

TABLE 8. Comparison of minerals and compounds related to markascherite

	Chemical formula	Space group	Unit-cell parameters (Å, °)	Reference	Main structure feature
Markascherite	$Cu_3(MoO_4)(OH)_4$	$P2_1/m$	$a = 9.990$, $b = 5.993$, $c = 5.526$, $\beta = 97.43$	1	brucite-type layers linked by MoO_4 and rutile-type chains
Szenicsite	$Cu_3(MoO_4)(OH)_4$	$Pnnm$	$a = 12.559$, $b = 8.518$, $c = 6.072$	2, 3	triple octahedral chains linked by MoO_4
Antlerite	$Cu_3(SO_4)(OH)_4$	$Pnma$	$a = 8.289$, $b = 6.079$, $c = 12.057$	4, 5, 6	triple octahedral chains linked by SO_4
Synthetic	$Cu_3(CrO_4)(OH)_4$	$Pnma$	$a = 8.262$, $b = 6.027$, $c = 12.053$	7	isotypic with antlerite
Synthetic	$Cu_3(SeO_4)OH_4$	$Pnma$	$a = 8.382$, $b = 6.087$, $c = 12.285$	8, 9	isotypic with antlerite
Flinkite	$Mn_2^{2+}Mn^{3+}(AsO_4)(OH)_4$	$Pnma$	$a = 9.483$, $b = 13.030$, $c = 5.339$	10, 11	octahedral layers with vacant sites, linked by AsO_4
Retzian	$Mn_2^{2+}REE^{3+}(AsO_4)(OH)_4$	$Pban$	$a = 5.67$, $b = 12.03$, $c = 4.863$	10	layers of MnO_6 and $REEO_8$ polyhedra, linked by AsO_4
Cahnite	$Ca_2B(AsO_4)(OH)_4$	$I\bar{4}$	$a = b = 7.11$, $c = 6.20$	12	3D network formed by CaO_8, BO_4, and AsO_4 sharing edges and corners
Chantalite	$CaAl_2(SiO_4)(OH)_4$	$I4_1/a$	$a = b = 4.952$, $c = 23.275$	13	$AlO_2(OH)_4$ octahedral chains linked by SiO_4 and CaO_8 polyhedra
Xocomecatlite	$Cu_3(TeO_4)(OH)_4$	?	$a = 12.140$, $b = 14.318$, $c = 11.662$	14	structure unknown
Deloryite	$Cu_4(UO_2)(MoO_4)_2(OH)_6$	$C2/m$	$a = 19.94$, $b = 6.116$, $c = 5.520$, $\beta = 104.18$	15, 16	brucite-type layers linked by MoO_4 and distorted UO_6
Derriksite	$Cu_4(UO_2)(SeO_3)_2(OH)_6$	$Pn2_1m$	$a = 5.570$, $b = 19.088$, $c = 5.965$	17	brucite-type layers linked by SeO_3 and distorted UO_6

Notes: References: (1) This work; (2) Burns (1998); (3) Stolz and Armbruster (1998); (4) Finney and Araki (1963); (5) Hawthorne et al. (1989); (6) Vilminot et al. (2003); (7) Pollack (1985); (8) Giester (1991); (9) Vilminot et al. (2007); (10) Moore (1967); (11) Kolitsch (2001); (12) Prewitt and Buerger (1961); (13) Liebich et al. (1979); (14) Williams (1975); (15) Tali et al. (1993); (16) Pushcharovsky et al. (1996); (17) Ginderow and Cesbron (1983).

extensive investigations owing to their intercalation chemistry, large potentially accessible internal surface area, and as precursors for the generation of two-dimensional nano-sheets (Ma et al. 2007; Mitchell et al. 2010, and references therein). The discovery of markascherite provides a new structure type for such research. Furthermore, based on the coupled substitution mechanism proposed above, it appears that various markascherite-type or deloryite-type layered compounds may be synthesized in laboratories or found in nature, such as $2Mn^{2+} \rightarrow 2Cu^{2+}$, $(Ti^{4+} + Mg^{2+}) \rightarrow (U^{6+} + \square)$, $2Al^{3+} \rightarrow (U^{6+} + \square)$, $(Ti^{4+} + \square + 2OH^{-}) \rightarrow (U^{6+} + \square + O^{2-})$, or $2Fe^{3+} \rightarrow (U^{6+} + \square)$.

Acknowledgments

This study was funded by the Science Foundation Arizona. Constructive comments and suggestions for improvement from I.E. Gray, F. Colombo, and an anonymous reviewer are greatly appreciated.

References cited

Alam, N. and Feldmann, C. (2010) The chain-like copper molybdate $[Cu(dien)]_2[MoO_4]_2 \cdot H_2O$. Zeitschrift für anorganische und allgemeine Chemie, 636, 437–439.

Bao, R., Kong, Z., Gu, M., Yue, B., Weng, L., and He, H. (2006) Hydrothermal synthesis and thermal stability of natural mineral lindgrenite. Chemical Research of Chinese Universities, 22, 679–683.

Brese, N.E. and O'Keeffe, M. (1991) Bond-valence parameters for solids. Acta Crystallographica, B47, 192–197.

Burns, P.C. (1998) The crystal structure of szenicsite, $Cu_3MoO_4(OH)_4$. Mineralogical Magazine, 62, 461–469.

Burns, P.C. and Hawthorne, F.C. (1996) Static and dynamic Jahn-Teller effects in Cu^{2+} oxysalt minerals. Canadian Mineralogist, 34, 1089–1105.

Crane, M., Frost, R.L., Williams, P.A., and Theo Kloprogge, J. (2002) Raman spectroscopy of the molybdate minerals chillagite (tungsteinian wulfenite-I4), stolzite, scheelite, wolframite and wulfenite. Journal of Raman Spectroscopy, 33, 62–66.

Downs, R.T., Bartelmehs, K.L., Gibbs, G.V., and Boisen, M.B. Jr. (1993) Interactive software for calculating and displaying X-ray or neutron powder diffractometer patterns of crystalline materials. American Mineralogist, 78, 1104–1107.

Eby, R.K. and Hawthorne, F.C. (1993) Structure relations in copper oxysalt minerals. I Structural hierarchy. Acta Crytallographica, B49, 28–56.

Finney, J.J. and Araki, T. (1963) Refinement of the crystal structure of antlerite. Nature, 197, 70.

Francis, C.A., Pitman, L.C., and Lange, D.E. (1997) Szenicsite, a new copper molybdate from Inca de Ora, Atacama, Chile. Mineralogical Record, 28, 387–394.

Frost, R.L., Duong, L., and Weier, M. (2004) Raman microscopy of the molybdate minerals koechlinite, iriginite and lindgrenite. Neues Jahrbuch für Mineralogie-Abhandlungen, 180, 245–260.

Frost, R.L., Bouzaid, J., and Butler, I.S. (2007) Raman spectroscopic study of the molybdate mineral szenicsite and comparison with other paragenetically related molybdate minerals. Spectroscopy Letters, 40, 603–614.

Giester, G. (1991) Crystal structure of synthetic $Cu_3(SeO_4)(OH)_4$. Monatshefte für Chemie, 122, 229–234.

Ginderow, D. and Cesbron, F. (1983) Structure da la derriksite, $Cu_4(UO_2)(SeO_3)_2(OH)_6$. Acta Crystallographica, C39, 1605–1607.

Hawthorne, F.C. and Eby, R.K. (1985) Refinement of the crystal structure of lindgrenite. Neue Jahrbuch für Mineralogie Monatshefte, 5, 234–240.

Hawthorne, F.C., Groat, L.A., and Eby, R.K. (1989) Antlerite, $Cu_3SO_4(OH)_4$, a heteropolyhedral wallpaper structure. Canadian Mineralogist, 27, 205–209.

Hermanowicza, K., Mączkaa, M., Wołcyrza, M., Tomaszewskia, P.E., Pacęciaka, M., and Hanuza, J. (2006) Crystal structure, vibrational properties and luminescence of $NaMg_3Al(MoO_4)_5$ crystal doped with Cr^{3+} ions. Journal of Solid State Chemistry, 179, 685–695.

Kolitsch, U. (2001) Redetermination of the mixed-valence manganese arsenate flinkite, $Mn^{II}_2Mn^{III}(OH)(AsO_4)$. Acta Crystallographica, E57, i115–i118.

Libowitzky, E. (1999) Correlation of O-H stretching frequencies and O-H···O hydrogen bond lengths in minerals. Monatshefte für Chemie, 130, 1047–1059.

Liebich, B.W., Sarp, H., and Parthe, E. (1979) The crystal structure of chantalite, $CaAl_2(OH)_4SiO_4$. Zeitschrift für Kristallographie, 150, 53–63.

Lucazeau, G. and Machon, D. (2006) Polarized Raman spectra of $Gd_2(MoO_4)_3$ in its orthorhombic structure. Journal of Raman Spectroscopy, 37, 189–201.

Lucazeau, G., Le Bacq, O., Pasturel, A., Bouvier, P., and Pagnier, T. (2011) High-pressure polarized Raman spectra of $Gd_2(MoO_4)_3$: phase transitions and amorphization. Journal of Raman Spectroscopy, 42, 452–460.

Luz-Lima, C., Saraiva, G.D., Souza Filho, A.G., Paraguassu, W., Freire, P.T.C., and Mendes Filho, J. (2010) Raman spectroscopy study of $Na_2MoO_4 \cdot 2H_2O$ and Na_2MoMo_4 under hydrostatic pressure. Journal of Raman Spectroscopy, 41, 576–581.

Ma, R., Liu, Z., Takada, K., Iyi, N., Bando, Y., and Sasaki, T. (2007) Synthesis and exfoliation of Co^{2+}-Fe^{3+} layered double hydroxides: An innovative topochemical approach. Journal of the American Chemical Society, 129, 5257–5263.

Maczka, M., Kojima, S., and Hanuza, J. (1999) Raman spectroscopy of $KAl(MoO_4)_2$ and $NaAl(MoO_4)_2$ single crystals. Journal of Raman Spectroscopy, 30, 339–345.

Mitchell, S., Gómez-Avilés, A., Gardner, C., and Jones, W. (2010) Comparative study of the synthesis of layered transition metal molybdates. Journal of Solid State Chemistry, 183, 198–207.

Montney, M.R., Thomas, J.G., Supkowski, R.M., Trovitch, R.J., Zubieta, J., and LaDuca, R.L. (2009) Synthesis, structure and magnetic properties of a copper molybdate hybrid inorganic/organic solid with a novel 10-connected three-dimensional network topology. Inorganic Chemistry Communications, 12, 534–539.

Moore, P.B. (1967) Crystal chemistry of the basic manganese arsenate minerals 1. The crystal structures of flinkite, $Mn^{2+}_2Mn^{3+}(OH)_4(AsO_4)$ and retzian, $Mn^{2+}_2Y^{3+}(OH)_4AsO_4$. American Mineralogist, 52, 1603–1613.

Pavani, K. and Ramanan, A. (2005) Influence of 2-Aminopyridine on the formation of molybdates under hydrothermal conditions. Europe Journal of Inorganic Chemistry, 2005, 3080–3087.

Pavani, K., Ramanan, A., and Whittingham, M.S. (2006) Hydrothermal synthesis of copper coordination polymers based on molybdates: Chemistry issues. Journal of Molecular Structure, 796, 179–186.

Pavani, K., Singh, M., Ramanan, A., Lofland, S.E., and Ramanujachary, K.V. (2009) Engineering of copper molybdates: Piperazine dictated pseudopolymorphs. Journal of Molecular Structure, 933, 156–162.

Pavani, K., Singh, M., and Ramanan, A. (2011) Oxalate bridged copper pyrazole complex templated Anderson-Evans cluster based solids. Australian Journal of Chemistry, 64, 68–76.

Pollack, S.S. (1985) Isomorphism of basic copper chromate $CuCrO_4 \cdot CuO \cdot 2H_2O$, and antlerite, $Cu_3(SO_4)(OH)_4$. Journal of Applied Crystallography, 18, 535–536.

Prewitt, C.T. and Buerger, M.J. (1961) The crystal structure of cahnite, $Ca_2BAsO_4(OH)_4$. American Mineralogist, 46, 1077–1085.

Pushcharovsky, D.Y., Rastsvetaeva, R.K., and Sarp, H. (1996) Crystal structure of deloryite, $Cu_4(UO_2)[Mo_2O_8](OH)_6$. Journal of Alloys and Compounds, 239, 23–26.

Robinson, K., Gibbs, G.V., and Ribbe, P.H. (1971) Quadratic elongation, a quantitative measure of distortion in coordination polyhedra. Science, 172, 567–570.

Sheldrick, G.M. (2008) A short history of *SHELX*. Acta Crystallographica, A64, 112–122.

Stolz, J. and Armbruster, T. (1998) X-ray single-crystal structure refinement of szenicsite, $Cu_3MoO_4(OH)_4$, and its relation to the structure of antlerite, $Cu_3SO_4(OH)_4$. Neues Jahrbuch für Mineralogie, Monatshefte, 1998, 278–288.

Tali, R., Tabachenko, V.V., and Kovba, L.M. (1993) Crystal structure of $Cu_4UO_2(MoO_4)_2(OH)_6$. Zhurnal Neorganicheskoi Khimii, 38, 1450–1452.

Tian, C., Wang, E., Li, Y., Xu, L., Hu, C., and Peng, J. (2004) A novel three-dimensional inorganic framework: hydrothermal synthesis and crystal structure of $CuMo_3O_{10} \cdot H_2O$. Journal of Solid State Chemistry, 177, 839–843.

Vilminot, S., Richard-Plouet, M., Andre, G., Swierczynski, D., Guillot, M., Bouree-Vigneron, F., and Drillon, M. (2003) Magnetic structure and properties of $Cu_3(OH)_4SO_4$ made of triple chains of spins $s = ½$. Journal of Solid State Chemistry, 170, 255–264.

Vilminot, S., Andre, G., Richard-Plouet, M., Bouree-Vigneron, F., and Kurmoo, M. (2006) Magnetic structure and magnetic properties of synthetic lindgrenite, $Cu_3(OH)_2(MoO)_4$. Inorganic Chemistry, 45, 10938–10946.

Vilminot, S., Andre, G., Bouree-Vigneron, F., Richard-Plouet, M., and Kurmoo, M. (2007) Magnetic properties and magnetic structure of $Cu_3(OD)_4XO_4$, X = Se or S: Cycloidal versus collinear antiferromagnetic structure. Inorganic Chemistry, 46, 10079–10086.

Williams, S.A. (1975) Xocomecatlite, $Cu_3TeO_4(OH)_4$, and tlalocite, $Cu_{10}Zn_6(TeO_3)(TeO_4)_2Cl(OH)_{25} \cdot 27H_2O$, two new minerals from Moctezuma, Sonora, Mexico. Mineralogical Magazine, 40, 221–226.

Xu, J. and Xue, D. (2007) Hydrothermal synthesis of lindgrenite with a hollow and prickly sphere-like architecture. Journal of Solid State Chemistry, 180, 119–126.

Xu, Y., Lu, J., and Goh, N.K. (1999) Hydrothermal assembly and crystal structures of three novel open frameworks based on molybdenum(VI) oxides. Journal of Materials Chemistry, 9, 1599–1602.

Yang, H., Sun, H.J., and Downs, R.T. (2011) Hazenite, $KNaMg_2(PO_4)_2 \cdot 14H_2O$, a new biologically related phosphate mineral, from Mono Lake, California, U.S.A. American Mineralogist, 96, 675–681.

Manuscript received May 25, 2011
Manuscript accepted September 22, 2011
Manuscript handled by Fernando Colombo